Solar Energy
and Sustainable Development
Refereed, biannual scientific journal issued by
The Libyan Center for Solar Energy Research and Studies

Enhanced Fuzzy MPPT Controller with Rules Compression for 10 kW Grid-Connected PV System

Hicham Stitou[1], Mohamed Amine Atillah[2], Abdelghani Boudaoud[3], Mounaim Aqil[4]

[1,2,3,4]Engineering and Applied Physics Team (EAPT), Superior School of Technology, Sultan Moulay Slimane University, Beni Mellal, Morocco.

E-mail: [1] hicham.stitou@usms.ma ,[2] mohamedamine.atillah@usms.ma, [3]abdelghani.boudaoud@usms.ma , [4]mounaim.aqil@usms.ma.

ARTICLE INFO

The 2nd International Conference on Materials Sciences and Mechatronics for Sustainable Energy and the Environment (MSMS2E 2025)
October 1-2, 2025 at EST-Béni Mellal- Morocco.

KEYWORDS

Power Grid; Fuzzy Logic Controller; MPPT; FLC.

ABSTRACT

This paper proposes an enhanced fuzzy logic controller (FLC) for photovoltaic (PV) systems, featuring a novel reduced-order design. It introduces a significantly simplified FLC for MPPT in a 10-kW grid-connected PV system. The proposed controller minimizes both the number of input variables and the number of membership functions (MFs). Specifically, it utilizes only a single input, the sum of conductance and its increment, and employs just five rules, a substantial reduction compared to the 25-49 rules typical in standard FLCs.

Integrated within a system architecture featuring a DC-to-DC converter and a 3-level voltage source converter (VSC) for grid power transfer via duty cycle control, this highly reduced FLC maintains robust MPPT performance through adaptive responses to varying weather conditions. Consequently, it achieves considerable simplification in implementation complexity without sacrificing operational efficiency. To our knowledge, this FLC is among the few controllers capable of such significant rule reduction while maintaining performance. Key results show that at 1 kW/m², incremental conductance (IC) achieves 99% efficiency compared to FLC's 96%. Under medium irradiance (0.5 kW/m²), FLC outperforms IC by 5% (93% vs. 88%). For low irradiance (0.2 kW/m²), both reach 95.2%.

* *Corresponding author.*

DOI: https://doi.org/10.51646/jsesd.v14i2.1208

Under large irradiance steps (0.4 to 1 kW/m^2), the FLC achieves 22× faster convergence than IC (0.015 s vs. 0.33 s),demonstrating superior dynamic response to abrupt solar variations. This highlights the proposed algorithm's robustness for dynamic weather scenarios while maintaining competitiveness in steady operation.

وحدة تحكم ضبابية محسنة لتتبع النقطة القصوى للطاقة مع تقليل القواعد لنظام كهروضوئي متصل بالشبكة بقدرة 10 كيلوواط

ستيتو هشام، عاطي الله، محمد أمين ، بوداود عبد الغني ، عاقل منعيم.

ملخص: تقترح هذه الورقة وحدة تحكم منطقية ضبابية (FLC) محسّنة لأنظمة الطاقة الشمسية الكهروضوئية(PV) ، تتميز بتصميم جديد. تقدم وحدة تحكم منطقية ضبابية مبسطة بشكل كبير لتتبع نقطة الطاقة القصوى (MPPT) في نظام كهروضوئي متصل بالشبكة بقدرة 10 كيلوواط. تقلل وحدة التحكم المقترحة من عدد متغيرات الإدخال وعدد دوال العضوية (MFs).على وجه التحديد، تستخدم إدخالًا واحداً فقط، وهو مجموع الموصلية وزيادتها، وتوظف خمس قواعد فقط، وهو تقليل كبير مقارنة بـ 25- 49 قاعدة نموذجية في وحدات التحكم المنطقية الضبابية القياسية. تظل وحدة التحكم المنطقية الضبابية المخفضة هذه، المدمجة ضمن بنية نظام تتميز بمحول DC-DC ومحول مصدر جهد ثلاثي المستويات (VSC) لنقل الطاقة إلى الشبكة عبر التحكم في دورة العمل، تحافظ على أداء قوي لتتبع نقطة الطاقة القصوى من خلال استجابات تكيفية لظروف الطقس المتغيرة. وبالتالي، فإنها تحقق تبسيطًا كبيرًا في تعقيد التنفيذ دون التضحية بالكفاءة التشغيلية. على حد علمنا، تمثل وحدة التحكم المنطقية الضبابية هذه واحدة من وحدات التحكم القليلة القادرة على هذا التخفيض الكبير في القواعد مع الحفاظ على الأداء. تظهر النتائج الرئيسية أنه عند 1 كيلوواط/م^2، تحقق طريقة الموصلية المتزايدة (IC) كفاءة 99٪ مقارنة بـ 96٪ لوحدة التحكم المنطقية الضبابية. تحت الإشعاع المتوسط (0.5 كيلوواط/م^2)، تتفوق وحدة التحكم المنطقية الضبابية على طريقة الموصلية المتزايدة بنسبة 5٪ (93٪ مقابل 88٪). بالنسبة للإشعاع المنخفض (0.2 كيلوواط/م^2)، تصل كلتا الطريقتين إلى 95.2٪. تحت خطوات الإشعاع الكبيرة (0.4 إلى 1 كيلوواط/م^2)، تحقق وحدة التحكم المنطقية الضبابية تقاربًا أسرع بـ 22 مرة من طريقة الموصلية المتزايدة (0.015 ثانية مقابل 33.0 ثانية)، مما يدل على استجابة ديناميكية فائقة للتغيرات الشمسية المفاجئة. يسلط هذا الضوء على قوة الخوارزمية المقترحة لسيناريوهات الطقس الديناميكية مع الحفاظ على القدرة التنافسية في التشغيل المستقر.

الكلمات المفتاحية: وحدة التحكم المنطقية الضبابية، تتبع النقطة القصوى للطاقة الشمسية، الشبكة الكهربائية.

1. INTRODUCTION

The global surge in energy demand has accelerated interest in renewable energy solutions, particularly photovoltaic, wind, and biomass systems [1]. Recent research has focused extensively on enhancing the efficiency and economic viability of these sustainable alternatives. Among renewable options, photovoltaic technology has demonstrated remarkable market penetration, outpacing other green energy sources with annual growth rates reaching 60% in recent years [2], [3]. This rapid adoption stems from PV's competitive advantages: abundant solar resources, declining implementation costs, and favorable policy frameworks that support clean energy initiatives worldwide. The increasing integration of PV systems into grids has heightened the demand for efficient MPPT techniques to optimize energy harvest under varying environmental conditions [4], [5].

Scientific literature classifies MPPT techniques into three main families, each presenting tradeoffs among simplicity, cost, accuracy, and robustness. The first category comprises conventional methods such as IC, P&O, and Hill Climbing (HC) [6]. Recognized for their conceptual simplicity and ease of implementation, they prove effective when irradiance and

temperature vary gradually. However, their performance degrades significantly under rapid changes or partial shading conditions. To overcome these challenges, researchers have developed advanced MPPT techniques based on soft computing that employ artificial intelligence (AI) and bio-inspired optimization methods to manage PV system nonlinearities and dynamic operating conditions effectively. The most prominent approach, Fuzzy Logic Control (FLC) [7], operates through intuitive IF-THEN rules rather than precise mathematical models, utilizing input parameters such as MPP tracking error, typically derived from dP/dV measurements, to dynamically regulate the DC-DC converter's duty cycle. This model-free architecture enables FLC to maintain robust performance during parametric variations and partial shading conditions, consistently outperforming conventional methods in locating the global MPP while handling data uncertainties effectively. However, FLC implementation requires careful design of membership functions and rule bases; an expertise-dependent process that can be computationally intensive. Other advanced soft computing techniques have been developed for MPPT applications, including artificial neural networks (ANNs) and nature-inspired metaheuristic algorithms such as the bat algorithm (BA), grey wolf optimizer (GWO), and particle swarm optimization (PSO). These are complemented by chaotic optimization methods that leverage nonlinear dynamics for enhanced search capabilities [8], all offering superior performance in complex environments at the cost of increased computational requirements compared to traditional approaches. Finally, the third category involves hybrid approaches. These methods aim to combine the strengths of conventional and soft computing approaches, namely PSO+P&O, ANN+IC, and ANN+FL [9], [10], [11]. The objective is to achieve robust, fast, and precise overall performance across a wide range of operating conditions while managing complexity. The ultimate choice of MPPT technique will therefore inherently depend on the specific requirements of the application, its environmental conditions, cost, and computational resource constraints.

Fuzzy logic-based MPPT controllers enable high tracking performance [12]. Historically, the majority of studies employed a system with two inputs and a single output, utilizing five membership functions (MFs) to create a total of 25 rules [13], while others employed 7 MFs, resulting in 49 rules, or 3 MFs for nine rules. Some previous approaches had already reduced complexity by using current variation as the sole input with only two MFs and two rules [14]. Although various inputs have been tested, temperature and irradiance variation, error variation, or momentum [15], power and voltage or current variations are often preferred for computational reasons [16]. In contrast to these approaches generally require at least two inputs, this work introduces an enhanced FLC for PV systems, featuring a novel reduced-order design. The proposed controller minimizes both input variables and MFs, resulting in a highly reduced FLC used to extract MPP from a 10-kW PV system connected to the grid. Notably, only the sole variable I/V + dI/dV is used as a single input with only five MFs. Consequently, the number of variables, the computation time, and the circuit complexity are considerably reduced, while also decreasing tracking speed and improving accuracy over other controllers.

The rest of this paper is structured as follows: Section II presents the methodology, detailing the PV panel modeling, fuzzy-based MPPT controller implementation, and power stage design,

including the DC-to-DC converter and a brief description of the three-level VSC; Section III evaluates the simulation results of the grid-connected PV system using the proposed MPPT approach, and Section IV concludes the paper.

2. METHODOLOGY AND MATERIALS

2.1. System description

The studied PV system comprises a 10-kW grid-connected PV array. It is constructed with seven parallel strings of SunPower SPR-305E-WHT-D modules, five modules per string. The system includes a DC-to-DC converter and a 3-level VSC with an LCL filter. The PV array, subject to irradiance ramping and temperature variations, delivers power to the converter. The latest steps up the DC voltage while an MPPT algorithm optimizes power extraction. The 3-level VSC converts the DC power to AC, with the LCL filter mitigating harmonics for grid compliance and local load supply. For grid interconnection, a 10-kVA isolation transformer boosts the inverter output from 260V to 25kV, matching the distribution feeder voltage that ultimately connects to a 120-kV bulk transmission network equivalent. The system architecture under study is depicted in Figure. 1.

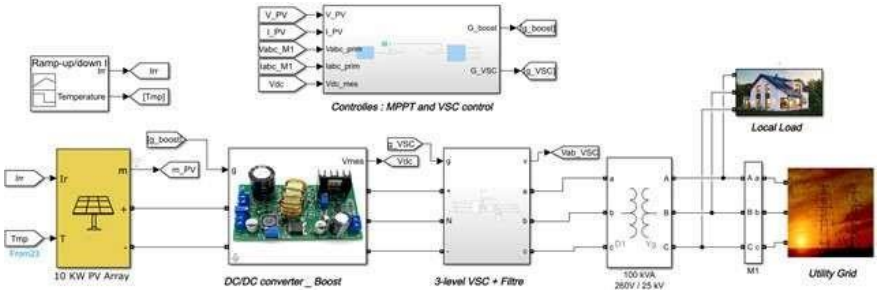

Figure. 1. Architecture of the studied system.

2.1.1. Model and characteristics of PV panels

This study employs the single-diode equivalent circuit model as shown in Figure. 2 to represent PV device behavior. The model consists of four key components: a photogenerated current source, a diode, a series resistor, and a shunt resistor, providing an optimal balance of simplicity and precision for PV system analysis [3].

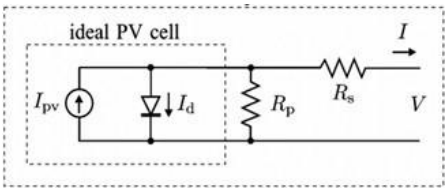

Figure. 2. Equivalent circuit of a solar cell.

Moreover, the total output current of the PV panel I is obtained using Kirchhoff's current law as shown in Eq. (1). PV array characteristics are shown in Figure. 3. I-V curves are shown in Figure. 3a for different values of irradiation. Figure. 3b shows I-V curves for different

temperatures. In Figure. 3c, P-V curves for different irradiations are presented, whereas in Figure. 3 d, P-V curves for different temperatures are illustrated.

$$I = I_{PV} - I_d - I_P \quad (1)$$

Where I_{PV} is the photocurrent, I_d is the current through the diode, and I_p is the current P-N junction of the diode.

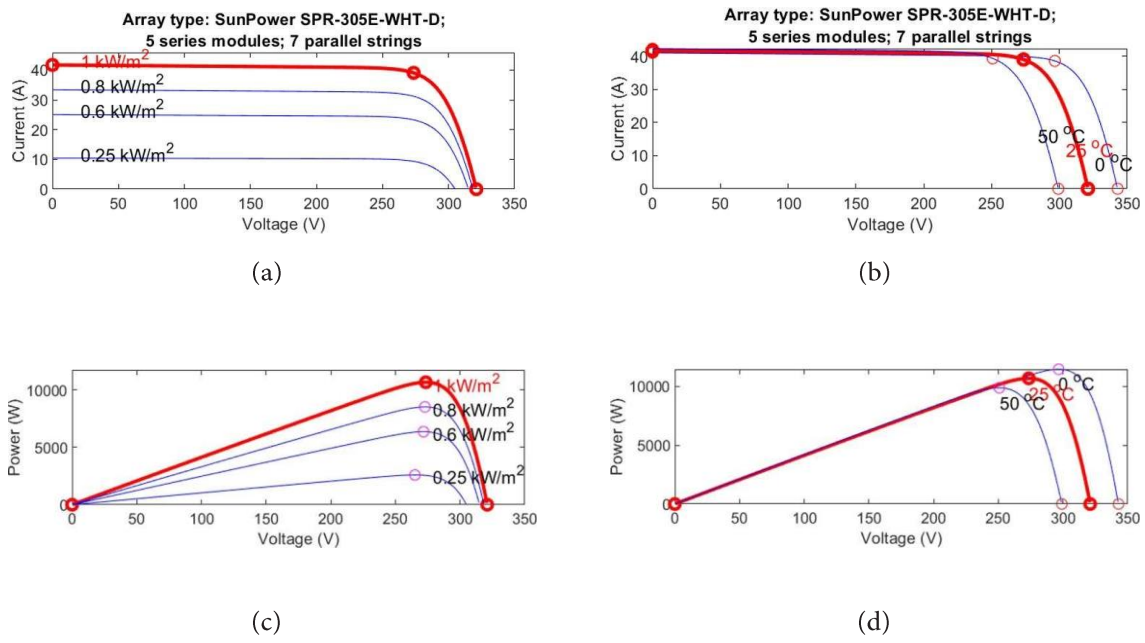

Figure. 3. (a) PV array I-V curves for different irradiations, (b) I-V curves for different temperatures, (c) P-V curves for different irradiations, (d) P-V curves for different temperatures.

The specifications for one PV module used in this study are detailed in Table 1.

Table 1: PV module specifications.

Number of series-connected cells	96
Open-circuit voltage and short-circuit current	Voc = 64.2 V, Isc = 5.96 A
Voltage and current at maximum power	Vmp =54.7 V, Imp= 5.58 A

2.2. Fuzzy-based MPPT controller

2.2.1. FL Controller structure

The FLC monitors the PV panel's voltage and current (I and V) to generate one fuzzy input variable. This input is processed through Mamdani's fuzzy inference system to calculate the optimal duty cycle command, which adjusts the PV system's operating point to maximize power extraction. As illustrated in Figure. 4, this calculation process follows a structured flowchart of FLC. The Mamdani FLC approach implements maximum power point tracking through four

sequential steps [17]: fuzzification of input variables, application of fuzzy rule base, fuzzy inference using compositional operators, and defuzzification to obtain the crisp duty cycle output. This method provides an effective balance between computational efficiency and control precision for PV systems.

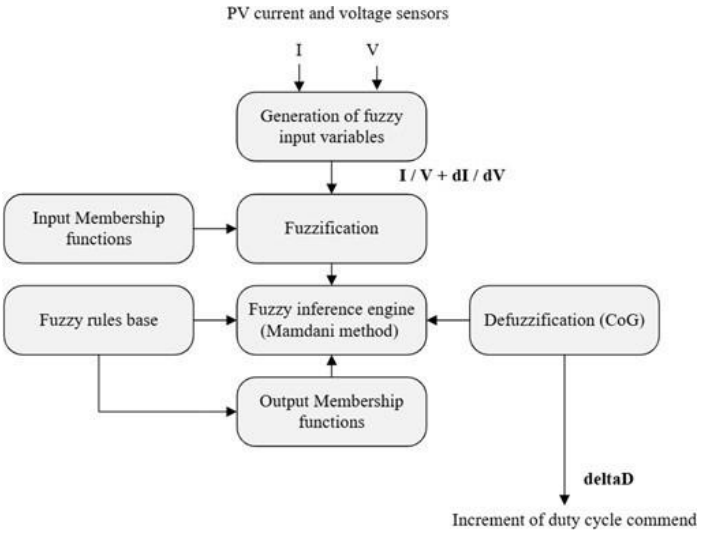

Figure. 4. Flowchart diagram of the fuzzy controller.

2.2.2. Fuzzy-based MPPT controller implementation

The proposed MPPT algorithm employs IC as the foundation for the fuzzy controller design. As demonstrated by the P-V curve characteristics and expressed in equations (2), (3), and (4), the power-to-voltage derivative dP/dV equals zero at the maximum power point (MPP), positive on the left of MPP, and negative on the right:

$$dP/dV = 0 \tag{2}$$

$$\Rightarrow I + V\,(dI/dV) = 0 \tag{3}$$

$$\Rightarrow I/V + dI/dV = 0 \tag{4}$$

The I-V characteristic is subdivided into three regions used to build a rules base, as shown in Figure.5a, and the corresponding major I Ú V+ dI Ú dV characteristic is presented in Figure. 5b. The proposed algorithm leverages this distinctive characteristic to design the fuzzy logic controller. A key feature of the approach is its ability to detect the operating point's position relative to the MPP on the P-V curve: when I Ú V+ dI Ú dV >0, the system operates on the left side of the MPP. Under this condition, indicating an excessively low PV output voltage, the controller intelligently reduces the duty ratio command to elevate the PV voltage toward the MPP. For I Ú V+ dI Ú dV <0, the controller increases the duty ratio to reduce excessive PV voltage. This single-input algorithm determines the operating region, with fuzzy rules shown in Table 2 and membership functions depicted by Figure. 6, enabling efficient MPPT.

The proposed algorithm directly locates the operating point relative to the MPP, unlike conventional methods that estimate MPP proximity through perturbations. This enables larger duty cycle adjustments for faster MPPT convergence while maintaining stability. The approach simplifies system design by requiring only single-input/single-output operation, reducing computational requirements. Its rule base is organized into three distinct operational regions for optimized tracking performance. Detailed analyses are provided below:

Region 1 (Right of MPP):

- The operating point resides on the right side of MPP on the P-V curve.
- The duty ratio is proportionally increased based on the measured distance to the MPP.

Region 2 (Near MPP):

- The operating point is close to the MPP.
- The output is maintained at Zero Error (ZE), indicating optimal power extraction.

Region 3 (Left of MPP):

- The operating point lies on the left side of the MPP.
- The duty ratio is proportionally decreased according to the detected deviation from the MPP.

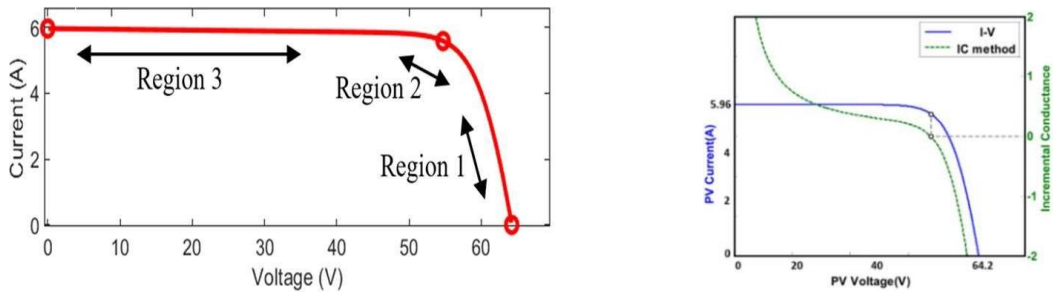

(a) (b)

Figure 5. (a) Operational regions, in I-V characteristic, to build a rules base and (b) the corresponding I/V+dI/dV.

The built and compressed fuzzy rule database for the proposed MPPT algorithm is shown in Table 2.

Table 2: Fuzzy rule database for FLC-based algorithm.

Input	NB	NS	ZE	PS	PB
Output	PB (↑↑)	PS (↑)	ZE (→)	NS (↓)	NB (↓↓)
Region	Region 1(Far Left)	Region 1(Near Left)	Region 2 (MPP)	Region 3 (Near Right)	Region 3 (Far Right)
Action	Large duty cycle increase	Small duty cycle increase	No change	Small duty cycle decrease	Large duty cycle decrease

This rule database uses five linguistic terms, namely positive small PS, positive big PB, zero ZE, negative big NB, and negative small NS for the input variable. The fuzzy controller adjusts the buck-boost converter's duty ratio, modifying the PV array's output voltage, which in turn updates the next input values. Careful design of input/output domains and membership

functions is critical, following a three-step process: (1) set PB/NB boundaries, (2) define ZE range based on MPPT goals, and (3) establish PS/NS boundaries iteratively.

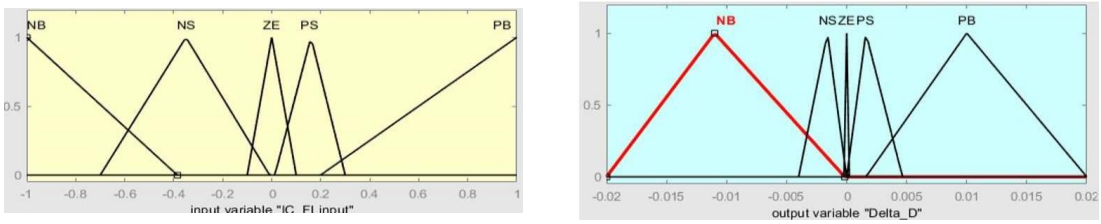

(a) (b)

Figure. 6. (a) Membership functions of input I/V + dI/dV, and (b) Membership function of output Delta_D.

The implementation diagram of the proposed fuzzy logic-based MPPT controller is illustrated in Figure. 7. This diagram includes an I/V and dI/dV computation block, which generates the combined input signal (I/V+dI/dV) for the FLC. This input is normalized before being processed by the FLC to produce the duty cycle adjustment output (Delta_D).

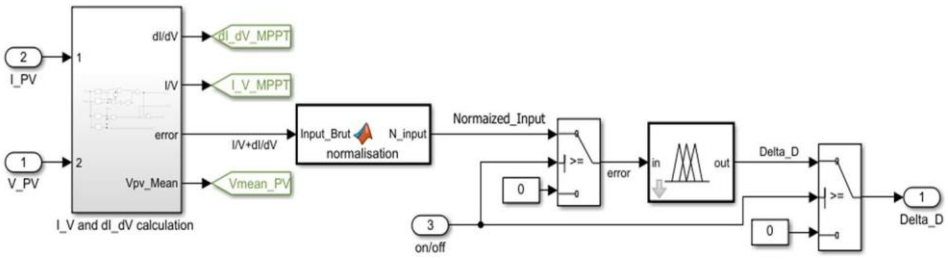

Figure. 7. Simulink diagram of MPPT-based Fuzzy logic controller.

2.3. Design of the DC-DC boost converter

The PV array supplies power to the boost converter while experiencing changing irradiance levels and temperature variations (Figure.1). It produces low voltages, typically requiring a series of connections for practical applications. The DC-DC boost converter increases voltage, reducing the number of series panels needed [4]. This optimizes cost and space while minimizing shading or panel degradation mismatch losses.

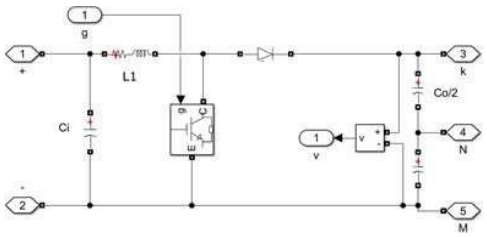

Figure. 8. Simulink diagram of DC-DC boost converter.

The converter uses PWM-based closed-loop control to maintain MPP operation by adjusting the duty cycle based on PV voltage (V) and current (I) measurements. MPPT algorithms optimize performance, while fast transient response handles irradiance or temperature changes. The diagram of the DC-DC boost is shown in Figure. 8.

The boost converter's input-output behavior is mathematically described by equation (5):

$$V_{out} = V_{in}/(1-D) \quad (5)$$

Where V_{in} is the input voltage, V_{out} is the output voltage, and D is the duty cycle.

Inductor and capacitor values are critical to balance ripple current and transient response. These values are obtained according to the equations used in [7]. In this simulation, the considered values of the designed components are as follows: Ci = 100 µF, Co = 24mF, and L1 = 5mH.

2.4. Three-level voltage source converter (VSC)

The three-level VSC converts the DC power to AC, with the LCL filter mitigating harmonics for grid compliance and local load supply (Figure. 1). Various multilevel inverter topologies exist in the literature, including diode-clamped, flying capacitors, and cascaded H-bridge configurations. Among these, the Neutral Point Clamped (NPC) topology [18], [19], [20] remains the most widely adopted. This work utilizes a three-level NPC-based Voltage Source Converter (VSC). It operates as follows: The three-phase VSC performs DC-AC conversion from 500 V to 260 V with unity power factor operation through a dual-loop control system: an outer loop regulating DC link voltage (±250 V) and an inner loop controlling grid current components (Id, Iq), where Id reference derives from the DC voltage controller and Iq is set to zero for unity PF. The current controller's Vd and Vq outputs are transformed into three-phase PWM signals (Uabc-ref) with 100 µs sampling for control loops and PLL synchronization, while the PWM generator operates at 1 µs resolution for precise switching.

3. RESULTS AND DISCUSSION

This section evaluates the performance of the developed MPPT algorithm under uniform irradiation conditions. The study employs a 10-kW grid-connected PV array system (Figure. 1) for testing and validation. To assess power tracking effectiveness between the PV panels and grid, we utilize a local load with the profile shown in Figure. 9a. The analysis is conducted at a constant temperature of 25°C across varying irradiation levels.

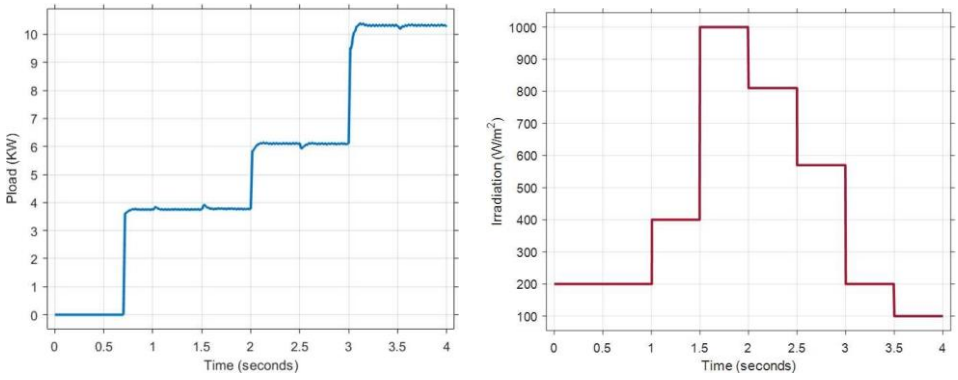

(a) (b)

Figure. 9. (a) Load profile used to evaluate the proposed MPPT method, and (b) Tested irradiation Levels.

To demonstrate the competitiveness and validity of the proposed MPPT-based FLC, a comparison of the designed controller with the conventional incremental conductance-based MPPT algorithm has been made for positive and negative irradiation steps, as depicted in Figure. 9b.

The panel power extraction compared to theoretical power, using the P-V characteristic, is illustrated in Figure. 10, where Figure. 10a displays the conventional IC algorithm's performance, and Figure. 10b shows the convergence behavior of this algorithm under abrupt irradiance changes. In contrast, Figure. 11a demonstrates the power capture of the proposed fuzzy-based MPPT, while Figure. 11b highlights its convergence time under the same step-irradiation conditions.

Simulation results demonstrate that for an abrupt irradiance change, from 0.4 to 1 kW/m², the fuzzy logic-based MPPT method achieves a remarkably fast convergence time (CT) of 0.015 s, compared to 0.33 s using the IC method, making it 22 times faster.

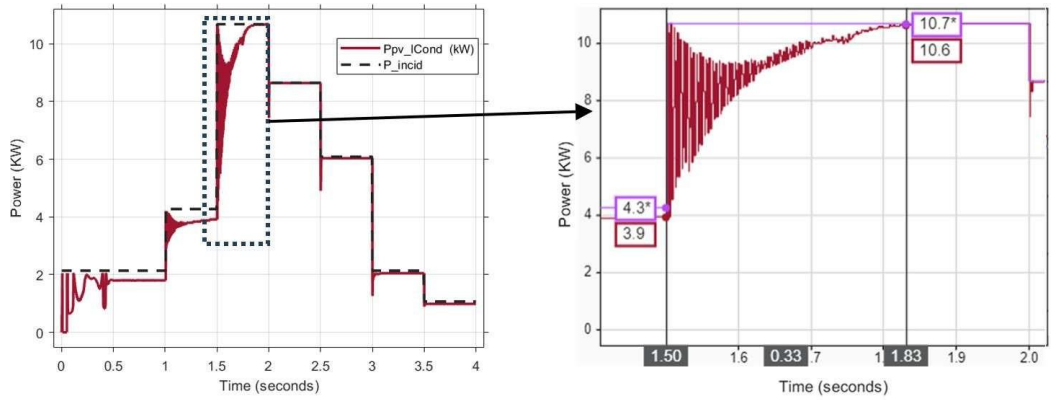

(a) (b)

Figure. 10. (a) Extracted PV power using the IC method, and (b) convergence time of PV Panel power.

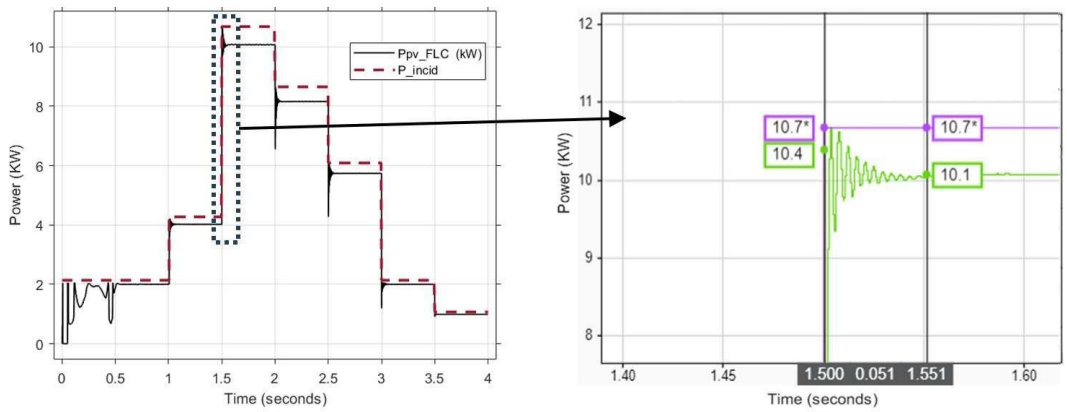

(a) (b)

Figure. 11. (a) Extracted PV power using the proposed fuzzy-based MPPT method, and (b) Convergence time of PV Panel power.

A comparison of efficiency and absolute error for the IC algorithm and the FLC method is reported in Table 3.

The efficiency values were derived from graphs presented in Figure. 10a and Figure. 10b. The efficiency values reveal distinct performance patterns for each MPPT method under varying irradiance conditions, as illustrated in Table 3: under standard conditions (1 kW/

m^2), IC achieves 99%, making it ideal for nominal operation, while FLC shows slightly lower 96% efficiency at full irradiance.

Table 3: Comparison of efficiency under 25 °C.

MPPT Method	Efficiency (%)	Absolute Error (%)
Incremental Conductance	99 % at 1 KW/m^2	1 %
	94.25 % at 0.8 KW/m^2	5.75 %
	98.36 % at 0.6 KW/m^2	1.64 %
	88.37 % at 0.4 KW/m^2	11.63 %
	95.24 % at 0.2 KW/m^2	4.76 %
Fuzzy Logic	96 % at 1 KW/m^2	4 %
	98.85 % 0.8 KW/m^2	1.15 %
	93.44 % at 0.6 KW/m^2	6.56 %
	93.02 % at 0.4 KW/m^2	6.98 %
	95.24 % at 0.2 KW/m^2	4.76 %

In partial irradiance conditions (0.2-0.8 kW/m^2), FLC demonstrates superior adaptability, performing 4.6% better at 0.8 kW/m^2 (98.85% vs. 94.25%) and maintaining more stable efficiency across mid-range irradiances (93-95%), whereas IC shows a significant 10.63% drop at 0.4 kW/m^2 (88.37% vs. FLC's 93.02%). Under low-light conditions (0.2 kW/m^2), both methods converge at an identical 95.24% efficiency. In conclusion, while the IC method performs well at high irradiance (1% error at 1 kW/ m^2), it exhibits significant error at low irradiance (11.63% at 0.4 kW/m^2). The FLC, however, demonstrates superior stability across the entire irradiance spectrum, with a maximum error of 6.98% at 0.4 kW/m^2, and proves more effective than IC at medium irradiance (1.15% vs. 5.75% error at 0.8 kW/m^2).

In the following part of this section, the analysis is focused on three operational regimes of the electrical grid in terms of active power flow: (i) balanced regime (Pload = Ppv), where consumption exactly matches photovoltaic production, (ii) underproduction regime (Pload > Ppv) requiring grid supplementation, and (iii) overproduction regime (Pload < Ppv) with surplus injection into the grid.

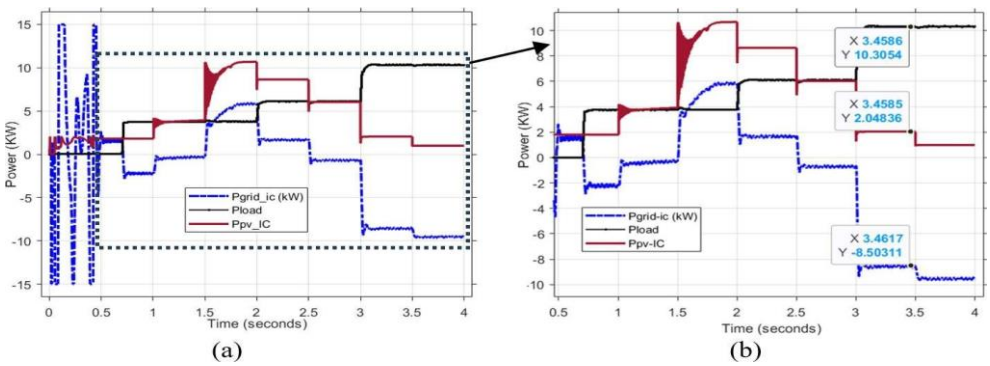

Figure.

12. (a) Grid power flow with IC MPPT method, and (b) Zoom from the instant of MPPT activation.

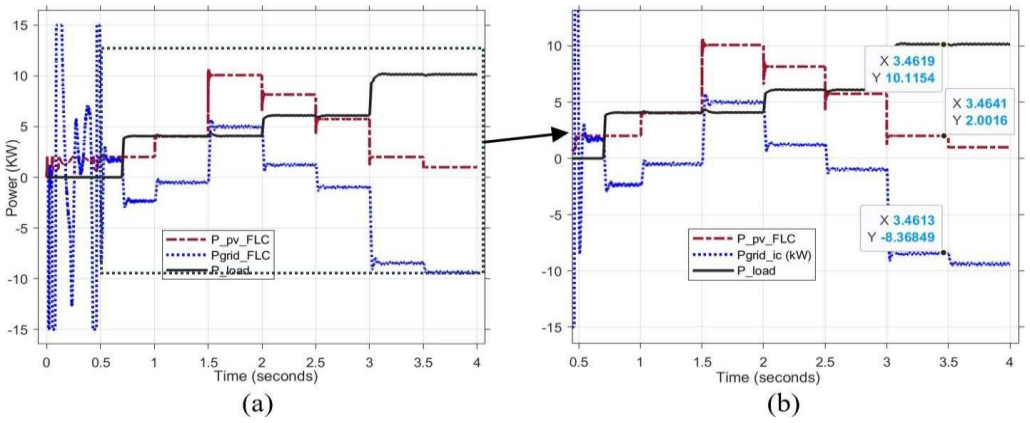

Figure. 13. (a) Grid power flow for the MPPT-based FLC method, and (b) Time-domain zoom from the MPPT algorithm activation instant.

Figure. 12 and Figure. 13, respectively, depict the power exchange between the grid, load, and PV system using the IC-based MPPT method and the proposed MPPT algorithm over a 4-second interval, enabling a comparative analysis.

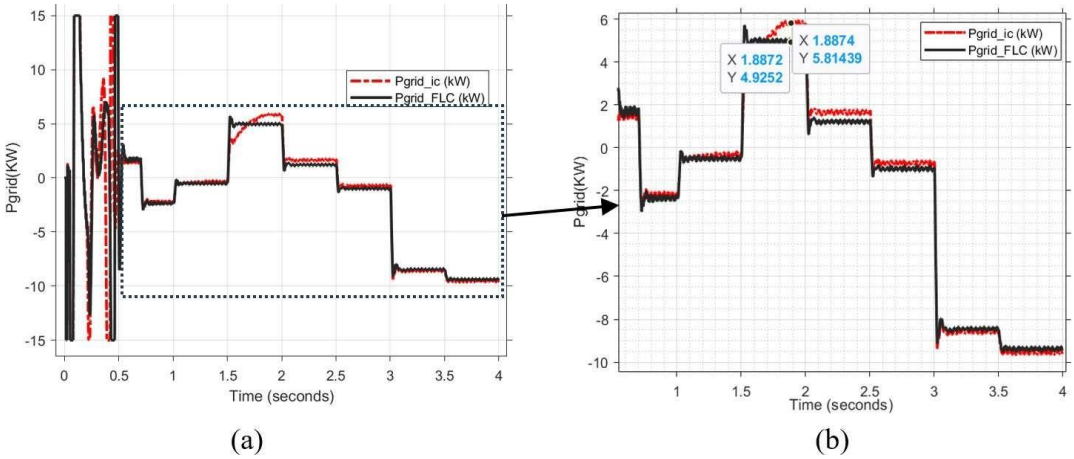

Figure. 14. (a) Grid power with two MPPT methods under different irradiation levels, and (b) Maximum power gain at 1 KW/m^2.

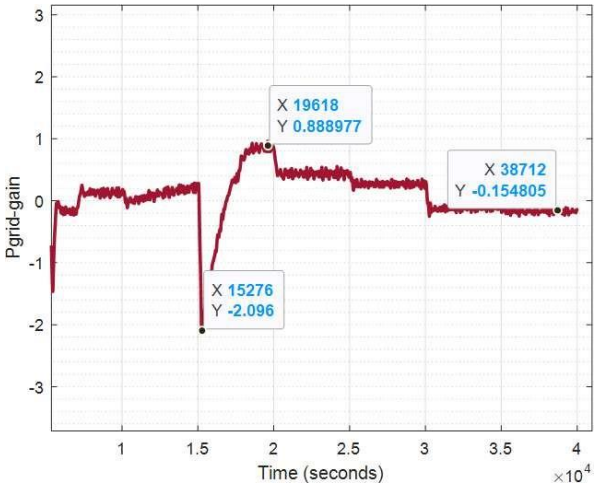

Figure. 15. Grid power gains between the two used MPPT algorithms.

The result of the simulation for grid active power using both the IC algorithm and the proposed fuzzy-based method is reported in Figure. 14. Figure. 14b shows a time domain zoom of Figure. 14a from the instant of activation of MPPT, maximum gain of approximately 0.9 KW at 1 KW/m2 is observed. Figure. 15 represents the grid power gain between the two MPPT algorithms used. This gain is defined as "Pgrid_gain=Pgrid_FLC - Pgrid_IC." Where Pgrid_FLC is the obtained grid power using fuzzy-based MPPT, and Pgrid_IC is the obtained grid power with the incremental conductance MPPT method.

As a conclusion from Figure. 15, the proposed algorithm demonstrates superior performance during transient states, particularly when handling large irradiation step changes. In contrast, the conventional IC method achieves better steady-state power output under stable conditions (1 kW/m² and 25°C), with a maximum gain of 0.89 kW. For minor irradiation fluctuations (0.1–0.2- 0.4 kW/m² and 25°C), the difference in power gain between both methods becomes negligible, not exceeding 0.155 kW. This highlights the proposed algorithm's robustness for dynamic weather scenarios while maintaining competitiveness in steady operation.

Table 4 presents a comparative analysis of the investigated MPPT methods (IC vs. FLC), quantifying their performance differences through metrics such as tracking efficiency (94–99% for IC vs. 95–98% for FLC), transient response, grid interaction, and complexity. The results reveal critical trade-offs, with IC favoring speed and FLC excelling in stability under irradiance fluctuations.

Table 4: Comparative performance analysis of IC vs. FLC MPPT algorithms.

Performance metric	IC MPPT	FLC MPPT	Remarks
Tracking speed (for small steps of irradiation)	Fast response	Slightly slower	IC reacts faster but may cause oscillations.
Stability	High oscillations during transients	Smooth power transitions	FLC excels in reducing grid stress.
Efficiency	~94–99% (nominal)	~95–98% (nominal)	Comparable under steady irradiance.
Grid Interaction	Sharp power injections/ withdrawals	Gradual power exchange	FLC favors grid stability.
Complexity	Low (model-based)	Low (FLC with rules compression)	Both are simpler to implement.

4. CONCLUSION

This study has successfully developed and validated a radically simplified single-input fuzzy logic MPPT controller for 10-kW grid-connected PV systems. By leveraging only the sum of conductance and its increment as input and operating with a drastically reduced set of just five rules, the controller achieves significant implementation simplification, 80-90% rule reduction, compared to conventional FLCs, without compromising efficiency. The results demonstrate superior dynamic performance, including 22 times faster convergence than Incremental

Conductance under faster irradiance steps and 5% higher efficiency at medium irradiance. This work confirms the feasibility of high-performance MPPT control with substantially reduced complexity.

Further work will analyze the operation of the controller in different environments as well as in the presence of partial shading. Its cost-effectiveness will be analyzed in the context of its implementation on inexpensive hardware platforms, as well as the cost-effectiveness for different system sizes. Some practical implementation issues, such as the choice of components, optimization of the switching losses, as well as noise immunity, will be considered. Improvements may be the use of adaptive modifications of the control rules or the use of this FLC in conjunction with other techniques for better performance in extreme situations.

Author Contributions: All authors have made significant and equitable intellectual contributions to this work. All team members participated in data interpretation, results validation, and approved the final manuscript.

Funding: This article received no external funding.

Data Availability Statement: All the data are available in the manuscript.

Acknowledgments: The authors gratefully acknowledge the support provided by the Engineering and Applied Physics Team (EAPT) at the Higher School of Technology, Sultan Moulay Slimane University, Beni Mellal, Morocco. The authors also sincerely appreciate the editor and reviewers for their timely observations and suggestions regarding this research article.

Conflicts of Interest: The authors declare that they have no conflicts of interest.

REFERENCES

[1] *M. Ali, M. Ahmad, M. A. Koondhar, M. S. Akram, A. Verma, and B. Khan, "Maximum power point tracking for grid-connected photovoltaic system using Adaptive Fuzzy Logic Controller," Comput. Electr. Eng., vol. 110, p. 108879, 2023, doi: https://doi.org/10.1016/j.compeleceng.2023.108879.*

[2] *S. Danyali, M. Babaeifard, M. Shirkhani, A. Azizi, J. Tavoosi, and Z. Dadvand, "A new neuro-fuzzy controller based maximum power point tracking for a partially shaded grid-connected photovoltaic system," Heliyon, vol. 10, no. 17, p. e36747, Sep. 2024, doi: 10.1016/j.heliyon.2024.e36747.*

[3] *S. J. Yaqoob, S. Motahhir, and E. B. Agyekum, "A new model for a photovoltaic panel using Proteus software tool under arbitrary environmental conditions," J. Clean. Prod., vol. 333, p. 130074, 2022, doi: https://doi.org/10.1016/j.jclepro.2021.130074.*

[4] *M. A. Atillah, H. Stitou, A. Boudaoud, M. Aqil, and A. Hanafi, "Study and analysis of partial shading effect on power production of a photovoltaic string controlled by three different MPPT techniques: P&O, PSO, and ANN," Math. Model. Comput., vol. 11, no. 3, pp. 856–869, 2024, doi: 10.23939/mmc2024.03.856.*

[5] *W. Alhosaini, M. Aly, E. M. Ahmed, and A. Shawky, "Optimized grid-connected three-phase photovoltaic inverter system using cascaded FOPIT-FOPI fractional controller," Energy Rep., vol. 13, pp. 3324–3339, Jun. 2025, doi: 10.1016/j.egyr.2025.02.055.*

[6] *N. E. Zakzouk, M. A. Elsaharty, A. K. Abdelsalam, A. A. Helal, and B. W. Williams, "Improved performance low-cost incremental conductance PV MPPT technique," IET Renew. Power Gener., vol. 10, no. 4, pp. 561–574, Apr. 2016, doi: 10.1049/iet-rpg.2015.0203.*

[7] *S. Bouri, O.-A. Mekkaoui, and A. M. Mamem, "Comparative Study of Different MPPT Methods of a Boost Chopper of PV Generator," Acta Electrotech. Inform., vol. 22, no. 3, pp. 24–31, Sep. 2022, doi: 10.2478/aei-2022-0014.*

[8] *F. Berttahar, S. Abdeddaim, A. Betka, and C. Omar, "A Comparative Study of PSO, GWO, and HOA Algorithms for Maximum Power Point Tracking in Partially Shaded Photovoltaic Systems," Power Electron. Drives, vol. 9, no. 1, pp. 86–105, Jan. 2024, doi: 10.2478/pead-2024-0006.*

[9] *S. Nawaz, "Design and Simulation of Improved Artificial Neural Netwok and Incremental Conductance HybridMPPT for Solar PV System Under Variable Irradiance Condition," pp. 1502– 1509, Jan. 2022, doi: 10.17051/ilkonline.2021.04.173.*

[10] *M. N. Ali, "Improved design of artificial neural network for MPPT of grid-connected PV systems," in 2018 Twentieth International Middle East Power Systems Conference (MEPCON), IEEE, 2018, pp. 97–102. doi: 10.1109/MEPCON.2018.8635202.*

[11] *M. Atillah, H. Stitou, A. Boudaoud, and M. Aqil, "Comparative Study of Two ANFIS-Based MPPT Controls under uniform and partial shading conditions," Sol. Energy Sustain. Dev., pp. 89–103, 2024. https://doi.org/10.51646/jsesd.v14iSI_MSMS2E.400*

[12] *M. M. Refaat, Y. Atia, M. M. Sayed, and H. A. Fattah, "Adaptive Fuzzy Logic Controller as MPPT Optimization Technique Applied to Grid-Connected PV Systems," in Modern Maximum Power Point Tracking Techniques for Photovoltaic Energy Systems, A. M. Eltamaly and A. Y. Abdelaziz, Eds., in Green Energy and Technology. , Cham: Springer International Publishing, 2020, pp. 247–281. doi: 10.1007/978-3-030-05578-3_9.*

[13] *J.-K. Shiau, Y.-C. Wei, and B.-C. Chen, "A study on the fuzzy-logic-based solar power MPPT algorithms using different fuzzy input variables," Algorithms, vol. 8, no. 2, pp. 100–127, 2015, doi: https://doi.org/10.3390/a8020100.*

[14] *J. Dadkhah and M. Niroomand, "Optimization Methods of MPPT Parameters for PV Systems: Review, Classification, and Comparison," J. Mod. Power Syst. Clean Energy, vol. 9, no. 2, pp. 225–236, Mar. 2021, doi: 10.35833/MPCE.2019.000379.*

[15] *B. N. Alajmi, K. H. Ahmed, S. J. Finney, and B. W. Williams, "Fuzzy-logic-control approach of a modified hill-climbing method for maximum power point in microgrid standalone photovoltaic system," IEEE Trans. Power Electron., vol. 26, no. 4, pp. 1022–1030, 2010, doi:10.1109/TPEL.2010.2090903.*

[16] *T. P. Kumar and B. N. Kartheek, "A neuro-fuzzy controller for multilevel renewable energy system," Indian J. Sci. Technol., vol. 9, no. 12, pp. 1–8, 2016, doi: 10.17485/ijst/2016/v9i12/72173.*

[17] *H. Stitou, M. amine Atillah, A. Boudaoud, and M. Aqil, "Load forecasting using fuzzy logic, artificial neural network, and adaptive neuro-fuzzy inference system approaches: application to South-Western Morocco," Int. J. Electr. Comput. Eng. IJECE, vol. 14, no. 6, Art. no. 6, Dec. 2024, doi: 10.11591/ijece.v14i6.pp7067-7079.*

[18] *P. Marish Kumar, N. Priya, R. Dhilipkumar, and T. Santhana Krishnan, "Maximizing solar energy eficiency with eficient interleaved boost converter with Three-Level neutral point clamped inverter for Grid-Connected photovoltaic using hybrid approach," Sol. Energy, vol. 280, p. 112855, Sep. 2024, doi: 10.1016/j.solener.2024.112855.*

[19] *S. K. Chattopadhyay and C. Chakraborty, "A New Asymmetric Multilevel Inverter Topology Suitable for Solar PV Applications With Varying Irradiance," IEEE Trans. Sustain. Energy, vol. 8, no. 4, pp. 1496–1506, Oct. 2017, doi: 10.1109/TSTE.2017.2692257.*

[20] *P. Ponnusamy et al., "A new multilevel inverter topology with reduced power components for domestic solar PV applications," IEEE Access, vol. 8, pp. 187483–187497, 2020, doi: 10.1109/ ACCESS.2020.3030721.*